Bulletin of JSME, Vol. 29, No. 254 August 1986

Paper No. 254—28

Natural Convection of Heat Generating Fluid within Horizontal Cylinder*

by Kohshi MITACHI,** Katsuyuki AOKI,***
Kenzo KITAMURA+ and Noritoshi KOMATSU++

The natural convection of a heat generating fluid within a horizontal cylinder has been studied analytically by solving the governing equations by a finite difference method. The rate of heat generation was assumed constant and distributed uniformly in the fluid. The surface temperature of the cylinder was considered isothermal. Computations were carried out on the case of Prandtl number Pr = 0.1, 1.0, 10 and 1000, and Rayleigh number from 10^2 to 10^8.

It was revealed that the velocity and temperature fields were little affected by Prandtl number in the range of Pr ≧ 1.0. The effect of natural convection on the heat transfer between the wall and fluid appeared at beyond Rayleigh number Ra = 10^4, and became dominant at Ra ≧ 10^6. Heat transfer experiments were also performed for the range of Ra = 3×10^3-10^9 by using a NaCl solution of 0.05 mol/kg water in concentration. The calculated average Nusselt numbers were in good agreement with the experiments.

Key Words : Convective Heat Transfer, Natural Convection, Internal Heat Generation, Horizontal Cylinder, Numerical Analysis, Experiment

1. Introduction

The problems of natural convection with internal heat generation are of considerable interest in many applications of heat transfer. A number of analytical and experimental studies have, therefore, been conducted to investigate the heat transfer behavior of the natural convection induced by a volumetric heat source. However, most of these works were concerned with the heat transfer between the horizontal plates [1-4], or in a cavity [5, 7, 8], while very few studies have been performed on the natural convection in a horizontal cylinder.

Jones [6] has first carried out the numerical analysis for the natural convection of a heat generating fluid confined in a horizontal cylinder. A gas mixture, which releases or absorbs the heat based on the Arreneus law, was adopted as a heat generating fluid. However, his analysis will not be of much use for further discussion, because only a limited range of Rayleigh number less than 4,000 was treated.

In spite of this, the studies concerning the horizontal cylinder are considered most important in view of the practical applications, in particular, to the field of nuclear technology. The reactions of nuclear fission and decay often take place in a storage vessel which contains the liquid suspensions of the nuclear fuels or of the radioactive waste. This reaction causes an internal heat generation and releases a large amount of heat. As one of these examples, a dump tank installed for a molten salt breeder reactor may be mentioned. This tank is used as the storage vessels of the fuel salt when an emergency shutdown of the reactor happens. A number of horizontal pipes or of bundles of the pipes are installed in the tank and the reacting salt is stored in them. Then, the outer surface of the pipes is cooled by an adequate cooling system in order to make the temperature of the fuel salt as low as possible. The natural convection appear in the pipes due to the temperature difference between the salt and the wall. The heat generated in the fuel salt is transported to the wall through natural convection. Therefore, the fundamental information about the flow and temperature fields within the horizontal pipes is indispensable to the design of these dump tanks.

Considering the above, in the present study is performed a numerical analysis of the natural convection of a heat generating fluid confined in a horizontal cylinder. The differential equations which describe the transport of heat and momentum and also the conservation of mass are numerically solved by using a finite difference method. To simplify the analysis, the rate of the heat generation is assumed to be constant and uniform throughout the fluid, and the inner surface of the cylinder is considered

* Received 17th October 1984
** Associate Professor,
*** Graduate Student, + Lecturer,
++ Under Graduate Student,
Toyohashi University of Technology,
Toyohashi, 440 Japan.

isothermal. The temperature and velocity distributions in the cylinder and also the local heat transfer coefficients between the wall and the fluid are obtained in the range of Rayleigh numbers up to 10^8.

Futhermore, heat transfer experiments are conducted and the results are compared with the above analytical results. A NaCl solution is adopted as a test fluid, and Rayleigh numbers range from 3×10^3 to 1×10^9 in the present experiments.

2. Analysis

2.1 Governing equations

The equations which govern the conservation of energy, momentum and mass are expressed as below in the cylindrical coordinate system, which is shown in Fig.1.

Energy equation:

$$V_r\frac{\partial T}{\partial R}+\frac{V_\phi}{R}\frac{\partial T}{\partial \phi}=\nabla^2 T+4 \quad \cdots\cdots\cdots\cdots(1)$$

Vorticity transport equation:

$$V_r\frac{\partial \Omega}{\partial R}+\frac{V_\phi}{R}\frac{\partial \Omega}{\partial \phi}=Pr\nabla^2\Omega + \frac{PrRa}{8}\left(\sin\phi\frac{\partial T}{\partial R}+\frac{\cos\phi}{R}\frac{\partial T}{\partial \phi}\right)\cdots\cdots(2)$$

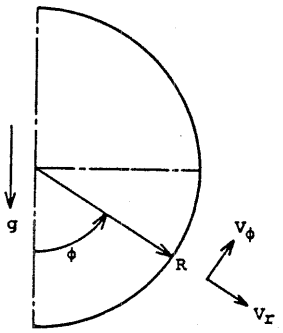

Fig.1 Coordinate system

Poisson equation for stream function:

$$\nabla^2\psi+\Omega=0 \quad \cdots\cdots\cdots\cdots\cdots\cdots(3)$$

where,

$$V_r=\frac{1}{R}\frac{\partial \psi}{\partial \phi}, \qquad V_\phi=-\frac{\partial \psi}{\partial R} \quad \cdots\cdots\cdots(4)$$

$$\nabla^2=\frac{\partial^2}{\partial R^2}+\frac{1}{R}\frac{\partial}{\partial R}+\frac{1}{R^2}\frac{\partial^2}{\partial \phi^2} \quad \cdots\cdots\cdots\cdots(5)$$

These equations are derived under the assumptions that the flow is laminar and two dimensional, and also that the thermophysical properties of the fluid are independent of temperature, except for the density in the buoyant term. In addition to these, the rate of heat generation is assumed constant and is distributed uniformly in the fluid.

The boundary conditions are written as:

$$T=0, \quad \psi=0, \quad \Omega=-\frac{\partial^2\psi}{\partial R^2} \quad \text{at } R=1 \quad \cdots\cdots\cdots\cdots(6)$$

$$\frac{\partial T}{\partial \phi}=0, \quad \psi=\Omega=0 \quad \text{at } \phi=0,\ \pi \quad \cdots\cdots\cdots(7)$$

The wall of the cylinder is supposed to be isothermal. The dimensionless variables in these equations are defined as follows:

$$\left.\begin{aligned} Pr&=\frac{\nu}{\alpha}, & R&=\frac{r}{r_w}\\ R_a&=\frac{g\beta t_0 d^3}{\nu\alpha}, & T&=\frac{t-t_w}{t_0}\\ t_0&=\frac{qr_w^2}{4\lambda}, & V_r&=\frac{v_r}{v_0}\\ V_\phi&=\frac{v_\phi}{v_0}, & V_0&=\frac{\alpha}{r_w}\\ \psi&=\frac{\psi'}{\alpha}, & \Omega&=\frac{\omega r_w^2}{\alpha} \end{aligned}\right\} \quad \cdots\cdots(8)$$

where,

- α : thermal diffusivity
- d : diameter of cylinder
- q : rate of heat generation
- r_w : radius of cylinder
- t_w : wall temperature of cylinder
- β : coefficient of volume expansion

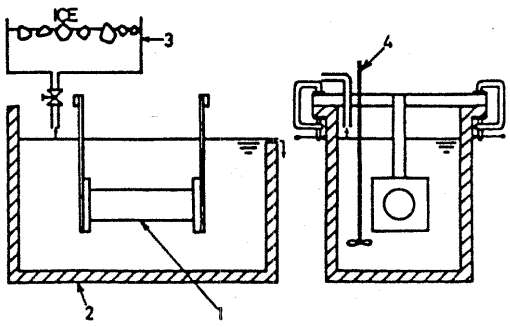

1 test cell 2 water bath
3 cooling water tank 4 stirrer

Fig.2 Experimental apparatus

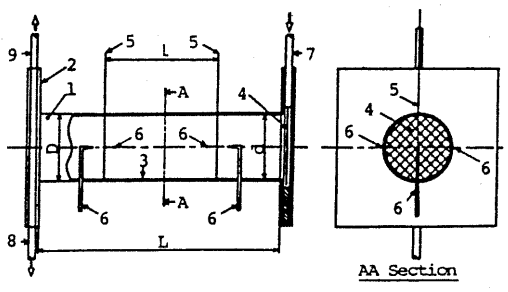

1 copper cylinder 2 acryl plate
3 insulation film 4 electrode
5 wire 6 thermocouple 7 fluid inlet
8 fluid outlet 9 air outlet

Fig.3 Test cell

λ : thermal conductivity
ν : kinematic viscosity
ψ' : stream function
ω : vorticity

2.2 Numerical procedure

The finite difference method is employed to obtain the solutions to the governing equations, Eq.(1)-(5), under the boundary conditions, Eq.(6)-(7). The central difference method is adopted to approximate the first order differential terms except for the convection term, which is approximated by an upwind difference method. Radial and circumferential increments are chosen as $\Delta r=1/21$ and $\Delta\phi=\pi/19$, respectively, which are determined in view of the convergence and the accuracy estimated from the test results for $Ra=10^6$.

The successive over relaxation (SOR) technique is used for the integration of the equations, Eq.(1)-(3). These equations are solved simultaneously by an iterative procedure, which consist of following main steps:

(i) The temperature at new time step are calculated by Eq.(1) using the known values of T_{ij}^{n-1}, V_{rij}^{n-1} and $V_{\phi ij}^{n-1}$.

(ii) By substituting the above temperatures T_{ij}^{n} into Eq.(2), the vorticities Ω_{ij}^{n} at a new step are estimated.

(iii) Then, the values of the stream function and the velocity components, V_{rij}^{n} and $V_{\phi ij}^{n}$, are computed by Eq.(3) and (4). These procedures (i), (ii) and (iii) are repeated until the maximum deviation between the values of Ω_{ij}^{n-1} and Ω_{ij}^{n} becomes less than 10^{-6}. About 40s CPU time is required for the case of $Ra=10^6$ on FACOM-M200 at Nagoya University.

3. Experiment

3.1 Experimental apparatus and measurements

Fig.2 is a schematical illustration of experimental apparatus. The apparatus consists of a test cell 1, a water bath 2, and a chilled water tank 3. The test cell is set in the water tank and the horizontal level is carefully adjusted. In order to maintain a constant temperature of the cell, chilled water is fed from the tank 3 and agitated by a stirrer 4.

The test cell is illustrated schematically in Fig.3. The copper cylinder 1 and the end plates 2 of acrylic plate constitute the cell. A NaCl solution of 0.05 mol/kg water in concentration fill the cell. A vinyl sheet 3 of 0.1mm thick glued on the inner surface of the cylinder insulates electrically the copper cylinder from the fluid. Stainless steel mesh screens of #24 mesh size are used as the electrodes 4 and are installed in the cylinder. AC power is supplied to the electrodes to generate heat in the fluid. The current supplied to the electrodes and

Table 1 Dimensions of test cell and experimental conditions

	d (mm)	l (mm)	D (mm)	L (mm)	Thickness of insulation layer (mm)	q (kw/m³)	Tc (°c)	Tl (°c)	Ra
Cell 1	8.0	46.0	20.0	50.	0.17	83-3000	22-41	21-28	$3*10^3$-$3*10^5$
Cell 2	20.1	150.0	22.2	250.	0.14	63- 380	22-28	21-23	$3*10^5$-$3*10^6$
Cell 3	41.0	150.7	45.0	250.	0.14	26- 180	27-33	26-28	$3*10^6$-$2*10^8$
Cell 4	102.0	150.0	114.6	350.	0.35	15- 53	17-23	14-16	$1*10^8$-$1*10^9$

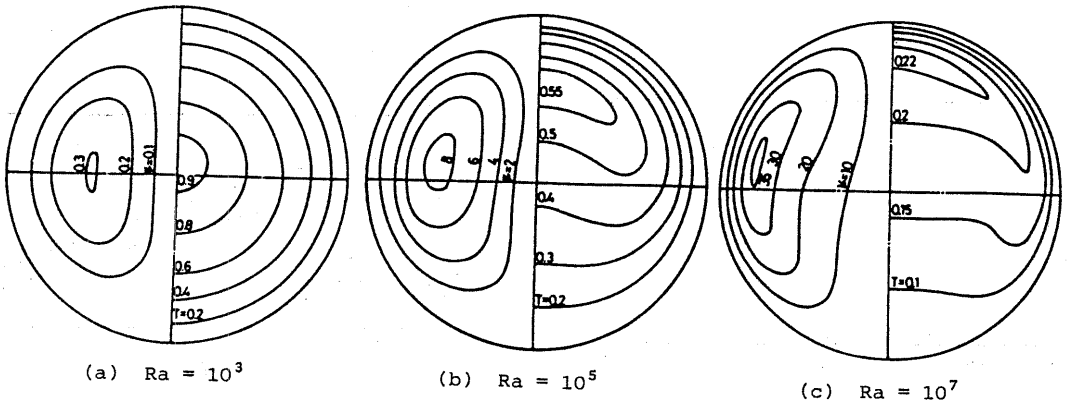

(a) $Ra = 10^3$ (b) $Ra = 10^5$ (c) $Ra = 10^7$

Fig.4 Distributions of temperatures and stream functions

voltage drop between the terminal wires 5 are recorded.

The temperature of the test fluid is measured with chromel-alumel thermocouples 6 of 0.1mm diameter, which are located at the central axis of the cell. These thermocouples are insulated electrically from the test fluid. The temperature of the cell is measured with four thermocouples 6 of 0.2mm diameter, which are welded to the outer surface of the copper cylinder.

After a steady state is attained, the values of the temperatures and of the input power are read. Another set of these data are collected after 20 minutes, and when both of the data were in good agreement, the data are employed. Four cells with different diameters are used to investigate the heat transfer characteristics in wide range of Rayleigh numbers. The dimensions of these cells and the relevant experimental conditions are tabulated in Table 1.

3.2 Heat generation rate and wall temperature

The rate of heat generation in the test fluid $q(w/m^3)$ is calculated by the following equation:

$$q = \frac{4IV}{\pi d^2 l} \quad \cdots\cdots\cdots\cdots\cdots\cdots\cdots\cdots(9)$$

where, I(A) is the electric current through the cell, and V(V) is the voltage drop between the two terminal wires which are l(m) apart from each other in the cell. The surface temperature of the vinyl sheet in contact with the fluid is extrapolated from the following equation. By using the temperature of the outer surface of copper cylinder t_1 and the thermal resistance of the vinyl sheet and copper, the equation is written as:

$$\left.\begin{aligned} t_w &= t_1 + R_{ow} IV \\ R_{ow} &= \frac{1}{2\pi l}\left(\frac{1}{\lambda_c}\ln\frac{r_{oc}}{r_{ic}} + \frac{1}{\lambda_v}\ln\frac{r_{ov}}{r_{iv}}\right) \end{aligned}\right\} \cdots(10)$$

where, r_{oc}, r_{ic}, and λ_c are the outer and inner diameters and the thermal conductivity of the copper cylinder, respectively. r_{ov}, r_{iv}, and λ_v are those of the vinyl sheet.

The values $(t_c-t_w)/(t_c-t_1)$ range from 0.45 to 0.80 in the present experiments, where t_c is the fluid temperature at the central axis of the cell.

4. Results and Discussion

4.1 Velocity and temperature distributions

As the representative data of the present analysis, the results will be presented for a fluid of Prandtl number Pr =10 in this paper.

Fig.4 shows the distributions of temperatures and stream functions in the cylinder at specific Rayleigh numbers. Fig.4(a) represents the results for the case of Rayleigh number 10^3. Here, the isotherms show concentric patterns, which implies that the heat is mainly transported through conduction.

The results for higher Ra numbers are given in Figs.4(b) and 4(c), where the isothermal lines become horizontal in the central portion of the cylinder. This is attributed to the natural convection induced in the cylinder.

the maximum stream function ψ_{max} is plotted against the Rayleigh number in Fig.5. Taking account of the fact that ψ_{max} increases as the velocity increases, the value of ψ_{max} is considered an indicator which describe the intensity of the recirculating flow in the cylinder. As is obvious from the figure, ψ_{max} increases monotonously with an increasing Ra number, but changes its gradient at around $Ra=10^4$. The maximum temperature Tmax ,and the mean temperatures Tb defined as follows are illustrated in Fig.6.

$$T_b = \frac{2\int_0^{r_w}\int_0^{\pi} T r d\phi dr}{\pi r_w^2} \quad \cdots\cdots\cdots\cdots(11)$$

Provided that the heat is transferred through conduction only, Tmax and Tb can

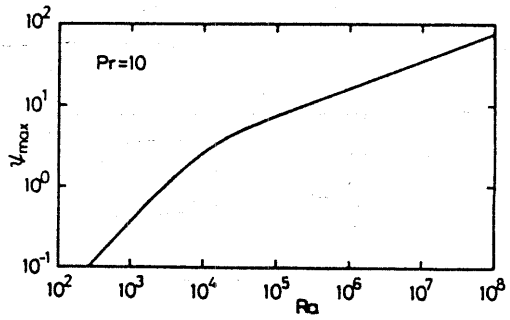

Fig.5 Maximum stream function

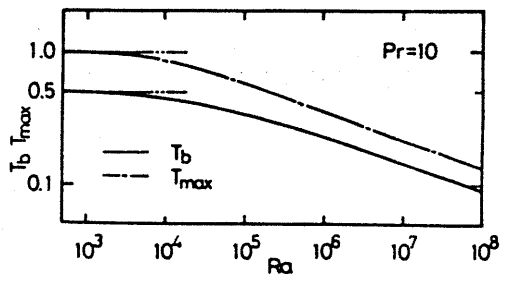

Fig.6 Maximum and mean temperature

be calculated easily and the results are presented with two dot chain lines in the figure. The figure shows that the numerical results of Tmax and Tb agree well with the above lines in the range of $Ra<5\times10^3$. At higher Rayleigh numbers, the values of Tmax and Tb becomes much smaller and the natural convection well explains this result. In the range of $Ra>10^6$, the maximum temperature Tmax can be correlated with the Ra numbers and is expressed as follows:

$$T_{max} \propto R_a^{-0.22} \quad \text{.....(12)}$$

4.2 Heat transfer coefficient

The local heat transfer coefficients h change their values with the azimuthal angle ϕ. The local Nusselt numbers defined as below are shown in Fig.7.

$$\left.\begin{aligned} q_w &= h(t_b - t_w) \\ N_u &= \frac{hd}{\lambda} \end{aligned}\right\} \quad \text{.....(13)}$$

As was mentioned in previous section, the natural convection induced in the cylinder is very weak in the case of $Ra=10^2$, and the heat is mainly transferred through conduction. Therefore, the Nu number remains constant at Nu=8.0, which coincides with that calculated by the pure conduction equation. On the other hand, the Nu number at $Ra=10^7$ depends strongly on ϕ. The Nu number at the top of the cylinder is six times larger than that at the bottom. The fluid lumps at high temperature ascend in the central portion of the cylinder and impinge on the top surface. Thus, the heat transfer is enhanced markedly here. At the bottom of the cylinder, temperature of a descending flow is reduced to an amount about equal to that of the cylinder wall, so that the Nu number will be decreased even though the convection motion becomes dominant. In the intermediate region of Ra numbers, $10^4<Ra<10^6$, the Nu number at $\phi=0$ is smaller than that calculated by pure conduction equation.

The local Nu number is integrated to yield the average Nusselt number Num defined by Eq.(14).

$$N_{um} = \frac{1}{\pi}\int_0^{\pi} N_u d\phi \quad \text{.....(14)}$$

Thus obtained Num is given in Fig.8 in terms of the Ra number. The figure indicates that the Num number coincides with that for the pure heat conduction at smaller Ra numbers. With an increase in Ra number, the Num number increases due to the natural convection. Furthermore, in the region of $Ra>10^6$, the Num number can be expressed by the following equation:

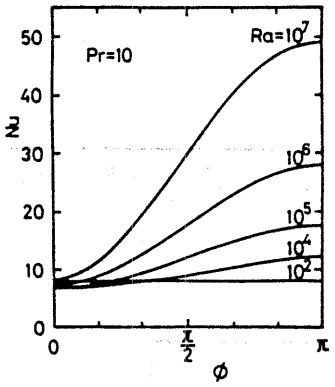

Fig.7 Local Nusselt number

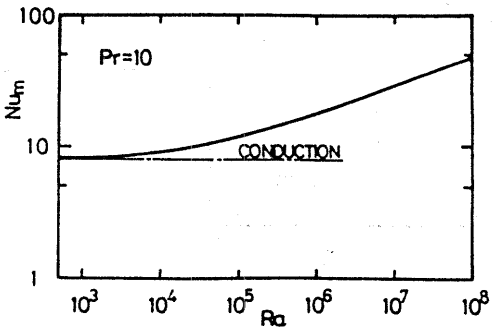

Fig.8 Average Nusselt number

Table 2 Effect of Prandtl number on average Nusselt number

Ra	Pr			
	0.1	1.0	10	1000
10^2	8.012	8.012	8.012	8.012
10^3	8.064	8.066	8.066	8.066
10^4	8.898	9.042	9.054	9.062
10^5	11.12	11.83	12.01	12.02
10^6	15.31	17.16	17.64	17.70
10^7	23.8	28.0	29.2	29.4
10^8			48.4	48.8

Table 3 Effect of Prandtl number on maximum temperature

Ra	Pr			
	0.1	1.0	10	1000
10^2	0.998	0.998	0.998	0.998
10^3	0.989	0.989	0.989	0.989
10^4	0.862	0.860	0.858	0.857
10^5	0.617	0.581	0.566	0.565
10^6	0.460	0.393	0.369	0.365
10^7	0.315	0.247	0.225	0.221
10^8			0.136	0.132

$$N_{um} \propto R_a^{0.22} \quad \text{.....(15)}$$

The exponent 0.22 in the above equation is almost equal to that obtained in the study of natural convection in a horizontal fluid layer [1,2,4].

The average Nusselt number Num and the maximum temperature Tmax of the fluid are also computed in the present study and the results are tabulated in Tables 1 and 2, respectively. The values of Num and Tmax for Pr=10 are almost the same as those for Pr=10^3, and well agree with those for Pr=1.0. Moreover, the results also reveal that the values of the mean temperature Tb and the maximum stream function ψ_{max} are scarcely affected by the Pr number of the fluid. Therefore, it is considered that the effects of Pr numbers on the temperature and velocity fields can be neglected in the practical applications, since the Prandtl numbers of molten salt in general range from 5 to 100.

4.3 Experimental results

In the previous sections, the heat transfer coefficient h is defined by using the temperature difference between the wall and the bulk fluid and is written as Eq.(13). However, it is hard to determine the bulk temperature experimentally, so that the average heat transfer coefficient h_e and the average Nusselt number Nue are defined as follows: They are based on the temperatures at the center of the cell t_c and at the wall t_w.

$$\left.\begin{aligned} h_e &= \frac{IV}{\pi dl}\frac{1}{t_c - t_w} \\ N_{ue} &= \frac{h_e d}{\lambda} \end{aligned}\right\} \text{.....(16)}$$

where, d is the inner diameter of the cell, and l is the distance between the two terminal wires.

The analytical Num numbers given in Fig.8 are, then, transformed into the above Nusselt number as follows:

$$N_{ua} = N_{um}\left(\frac{Tb}{Tc}\right) \quad \text{.....(17)}$$

where, Tb and Tc are dimensionless temperatures at the bulk and the center of the cylinder, respectively. The ratio Tb/Tc are plotted against Ra numbers in Fig.9.

The average Nusselt number, which is based on the temperatures Tc and Tw, is illustrated in Fig.10. The solid line in the figure indicates the Nua-Ra correlation obtained from the analysis and the broken line shows the Nua numbers, which are extrapolated from the above results. The vinyl sheet glued on the inner surface of the cylinder, causes a thermal resistance to the heat flow. Therefore, some corrections should be made to the experimental data. The thermal conductivity

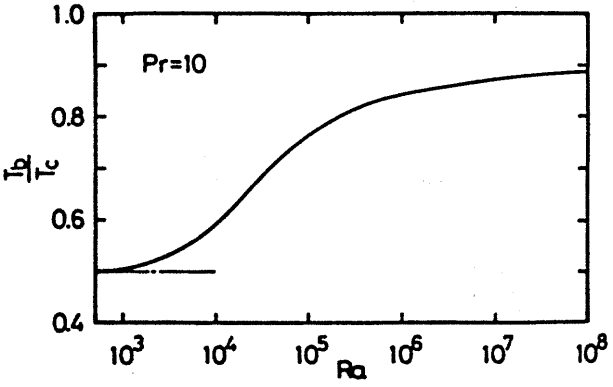

Fig.9 Relation between Tb/Tc and Ra

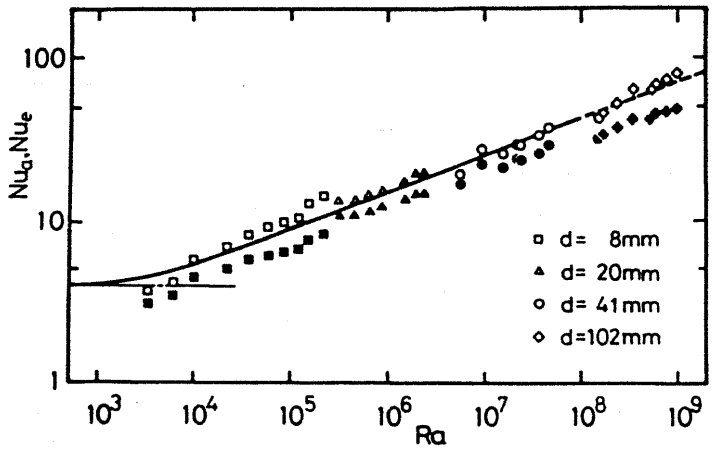

Fig.10 Average Nusselt number
(numerical and experimental result)

of the vinyl sheet λv is expected to fall within the range of 0.12 to 0.24 W/mK [10]. The open and solid symbols in the figure represent the Nue numbers calculated with values of λv of 0.12 and 0.24 W/mK, respectively. The NaCl solution of 0.05 mol/kg water in concentration was utilized in the present experiment. The above concentration is low enough, so that the thermophysical properties of the solution are considered the same as those for water. Therefore, they are estimated from the values for water and the film temperature Tf=(Tw+Tc)/2 is chosen as the reference temperature. As is apparent from the figure, a similar dependency of Nusselt numbers on the Rayleigh number is recognized between the analysis and the experiment, although some differences less than 30% are observed. The reason for those differences are due, in part, to the incorrect estimation of the thermophysical properties for the vinyl sheet and for the test fluid.

5. Conclusions

A numerical study has been conducted to investigate the natural convection heat transfer of a heat generating fluid, which is confined in a horizontal cylinder. The outer surface of the cylinder is cooled isothermally.

Heat transfer experiments are also performed in the range of Rayleigh numbers, $3\times10^3<Ra<10^9$. The NaCl solution is adopted as a test fluid. the following conclusions are obtained from these studies:

(1) In the range of Rayleigh numbers, $Ra<10^4$, the heat transfer coefficients are in good agreement with those estimated from the pure conduction equation. Most of heat is, therefore, transferred through conduction. The natural convection exerts influence on heat transfer rates and the maximum temperature when the Rayleigh number are larger than 10^4.

(2) The average Nusselt number Num and the maximum non-dimensional temperature Tmax are scarcely affected by Prandtle number in the range of Pr>5.

(3) Natural convection becomes dominant at $Ra>10^6$. Here, the average Num numbers increase in proportion to $Ra^{0.22}$, and the values of Tmax decrease in proportion to $Ra^{0.22}$.

(4) The numerical technique adopted in the present study can predict the heat transfer behavior of high Rayleigh number flows up to $Ra=10^8$. It is found that the analytical results well explain the experimental data.

Acknowledgement

The authors wish to express their thanks to Prof. Y. Iida, Yokohama National University, for his valuable suggestions and discussions throughout the study.

References

1. Kulacki, F.A. and Emara, A.A., J. Fluid Mech., Vol.83, No.2 (1977) p.375.
2. Cheung, F.B., Int. J. Heat & Mass Transfer, Vol.20, No.5 (1977) p.499.
3. Emara, A.A. and Kulacki, F.A., Trans. Amer. Soc. Mech. Engrs., J. Heat transfer, Vol.102, No.3 (1980) p.531.
4. Kikuchi, Y., et al., Int. J. Heat & Mass Transfer, Vol.25, No.3 (1982) p.363.
5. Watson, A., J. Mech. Eng. sci., Vol.13, No.3 (1971) p.151.
6. Jones, D.R., Int. J. Heat & Mass Transfer, Vol.16, No.1 (1973) p.157.
7. Kee, R.J., et al., Trans. Amer. Soc. Mech. Engrs., J. Heat Transfer, Vol.98, No.1 (1976) p.55.
8. Bergholz, R.F., Trans. Amer. Soc. Mech. Engrs., J. Heat Transfer, Vol.102, No.2 (1980) p.242.
9. Mitachi, K., et al., Prepr. Japan Soc. Mech. Engrs. (in Japanese), No.922 (1983) p.178.
10. Japan Soc. Chem., Kagaku Binran -ohyohhen- (in Japanese), (1980) p.809, Maruzen.